Springer

KSME

Journal of Mechanical Science and Technology 24 (8) (2010) 1729~1735
www.springerlink.com/content/1738-494x
DOI 10.1007/s12206-010-0519-9

Crosstalk calibration for torque sensor using actual sensing frame †

Young-Loul Kim, Jung-Jun Park and Jae-Bok Song*

School of Mechanical Engineering, Korea University, Seoul, 136-713, Korea

(Manuscript Received June 5, 2009; Revised February 24, 2010; Accepted May 13, 2010)

Abstract

Accurate load sensing is crucial to robots' performance of various tasks undertaken to assist workers. Most of the research on load sensing by robot manipulators has focused on improving force/torque sensor hardware. Torque sensors suffer from crosstalk, which cannot be compensated, not even through calibration. Thus, for minimization of crosstalk, torque sensors require precise machining and a complicated structure, which often increase costs. This paper proposes an alternative, novel calibration method. In this scheme, first, the compliance matrix of the torque sensor is obtained from sampling data, and then the location and scale of the actual sensing frame, in which crosstalk-free load sensing occurs, can be estimated. Using the proposed calibration method, the external load acting on the end-effector can be sensed accurately, even with relatively low-quality torque sensors. Experimental results show that measurement accuracy was significantly improved with the proposed method.

Keywords: Torque sensor; Calibration; Crosstalk; Manipulator

1. Introduction

A service robot's accurate sensing of external loads at the manipulator's end-effector is crucial to its successful performance, particularly as such systems are employed to assist workers in various precision tasks [1, 2]. Because commercially available force/torque sensors, due to their high cost and size, are not suitable for service robots, load sensing must be accomplished by means of relatively inexpensive load sensors.

Various methods have been used to measure external loads applied to robot arms. Among them, six-axis force/torque sensors [3-5] and joint torque sensors are popular. The six-axis force/torque sensor, frequently mounted at the wrist of the manipulator, can accurately measure the external load acting on the end-effector. However, since its structure is very complicated, it is too expensive to be employed in practical service robots. Instead, joint torque sensors are usually used in practical manipulators.

The joint torque sensor requires calibration for accurate sensing. The typical calibration methods are compliance matrix, as computed by structural analysis [6], the least-squares method [5], and the approach based on robot arm motion [7, 8]. However, crosstalk caused by forces other than the target force of the sensor cannot be compensated by such methods. Therefore, most torque sensors are designed to minimize crosstalk by structural analysis [9-12]. In most cases though, such crosstalk problems cannot be avoided, due to machining errors and misalignment of strain gauge bonding. A recent paper suggested a calibration method that can reduce crosstalk error using virtual load [13]. But not even this method is a totally satisfactory solution.

In this calibration method, the compliance matrix of a nominal sensing frame is obtained from sampling data, and then the location and scale of an actual sensing frame in which the load without crosstalk can be measured, are estimated. In this way, the true external load without crosstalk can be measured.

The main contribution of this proposed calibration method is the provision of accurate external load data by means of inexpensive load sensors or custom-designed low-accuracy sensors of simple structure.

The rest of this paper is organized as follows. The concept of crosstalk related to the joint torque sensor is introduced in Section II. The proposed calibration method that uses the actual sensing frame is detailed in Section III. The scheme's experimental verification is treated in Section IV. Finally, conclusions are drawn and future work is outlined in Section 5.

2. Error analysis of force/torque sensing

2.1 Crosstalk phenomenon

When a specified force (or torque) applied to the object is to be measured using a strain gauge, other forces (or torques)

† This paper was recommended for publication in revised form by Associate Editor Jong Hyeon Park
* Corresponding author. Tel.: +82 2 3290 3362, Fax: +82 2 3290 3757
E-mail address: jbsong@korea.ac.kr

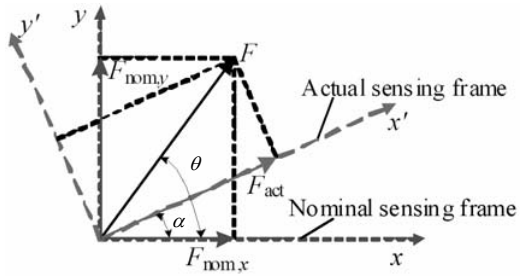

Fig. 1. Sensed torque by actual and nominal sensing frames.

acting on that object affect the sensor output as well. The sensor response to those unwanted loads is called *crosstalk*. Crosstalk has an adverse effect on the force/torque sensor accuracy. The amount of crosstalk can be described by

$$z = C_t F_t + C_u F_u \tag{1}$$

where z is the sensor output, F_t is the target force to be measured, F_u is the unwanted force, and C_t and C_u are the scale factors associated with F_t and F_u, respectively. Only in the ideal case where the sensor does not respond to F_u (i.e., no crosstalk) or $F_u = 0$, the target force F_t can be obtained accurately from the sensor output z in Eq. (1).

Force/torque sensor crosstalk is caused mainly by the error involved in either inaccurate strain gauge bonding or imprecise machining of the surface to which a strain gauge is attached [13]. In other words, the nominal sensing frame in which the sensor is supposed to generate the force (or torque) components is not consistent with the actual sensing frame in which the sensor actually generates the force (or torque) components. To understand this situation, consider the example of a force sensor below

Suppose the external force F is applied to an object in which a force sensor is installed. If the force sensor were correctly installed, the target force $F_{\text{nom},x}$ could be accurately measured from the force sensor output. In this ideal case, the y-axis component of the applied force, $F_{\text{nom},y}$, does not affect the sensing of the target force, and so there is no crosstalk. In actual implementation, however, the actual force sensor is inevitably affected by crosstalk from $F_{\text{nom},y}$. Therefore, the force sensor output z can be described by the linear combination of the target force, $F_{\text{nom},x}$, and the unwanted force, $F_{\text{nom},y}$, as follows:

$$z = C_1 F_{\text{nom},x} + C_2 F_{\text{nom},y} = F(C_1 \cos\theta + C_2 \sin\theta) \tag{2}$$

where C_1 and C_2 are the scale factors associated with the force components in the x and y axes. When the scale factors are replaced by

$$\gamma = \sqrt{C_1^2 + C_2^2}\ , \quad \alpha = \text{atan2}(C_2, C_1)\ ,$$

Eq. (2) becomes

$$z = \gamma F \cos(\theta - \alpha) = \gamma F_{\text{act}} \tag{3}$$

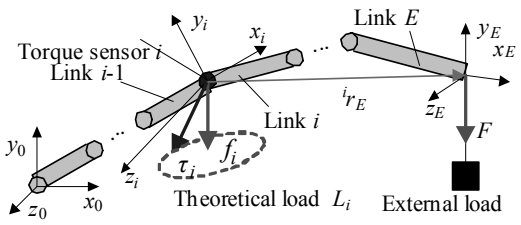

Fig. 2. Free body diagrams for serial manipulator.

where F_{act} denotes the actual force sensed by the force sensor. In Fig. 1, the x'-axis in the actual sensing frame is rotated α in the counterclockwise sense from the x-axis in the nominal sensing fame. Note that the sensor output z is the proportional to the force componen F_{act} in this x'-axis without crosstalk from other forces.

2.2 Comparison with virtual load method

To improve the measurement accuracy of low-cost sensors for a manipulator, crosstalk calibration using a virtual load was suggested in the previous research [13]. This paper proposes a novel crosstalk calibration scheme using an actual sensing frame. The two methods are compared in detail below.

Two approaches can be considered to deal with the crosstalk problem in Eq. (1). The first approach compensates for crosstalk by obtaining the force component F_u that causes the crosstalk and eliminating it ($C_u \rightarrow 0$). The second approach compensates for crosstalk by making the coefficient C_u zero. The above mentioned virtual load method [13] is based on the first approach, whereas the proposed method on the second approach.

3. Proposed calibration method

The crosstalk of a torque sensor discussed in the previous section cannot be compensated by means of the general calibration methods. Thus, a novel calibration method for compensating this crosstalk is proposed here.

3.1 Calculation of compliance matrix

Consider the six-link serial manipulator with 6 revolute joints shown in Fig. 2. Assume that each link frame is assigned at the proximal joint of each link and that torque sensor i (i = 1, ···, 6) is installed at each joint i. Suppose external load F is applied to endpoint E.

Now, consider the free body diagrams shown in Fig. 2. From the force and moment balance, the theoretical load L_i applied to each torque sensor can be computed from the known external load F as follows:

$$f_i = {}^iR_E \cdot F \tag{4}$$

$$\tau_i = {}^ir_E \times ({}^iR_E \cdot F) = {}^ir_E \times f_i \tag{5}$$

where f_i and τ_i are the internal force and torque vector applied to torque sensor i, respectively, and ${}^iR_E$ is the rotation matrix

describing the end-effector frame $\{E\}$ relative to the joint frame $\{i\}$, which is the nominal sensing frame, and ${}^{i}r_{E}$ is the position vector of the origin of the end-effector frame relative to the joint frame $\{i\}$. Note that the theoretical load applied to each joint torque sensor actually corresponds to the internal force and torque.

The theoretical load vector associated with joint torque sensor i can be described by

$$L_i = [f_i \ \tau_i] = [f_{xi} \ f_{yi} \ f_{zi} \ \tau_{xi} \ \tau_{yi} \ \tau_{zi}]^T \tag{6}$$

where f_{xi}, f_{yi}, f_{zi}, τ_{xi}, τ_{yi}, and τ_{zi} are the force and torque components of the theoretical load vector in the nominal sensing frame. The relationship between the theoretical load L_i and the sensor output z_i of torque sensor i can be described by

$$z_i = C_i \cdot L_i = [C_{f_{xi}} C_{f_{yi}} C_{f_{zi}} C_{\tau_{xi}} C_{\tau_{yi}} C_{\tau_{zi}}] \begin{bmatrix} f_{xi} \\ f_{yi} \\ f_{zi} \\ \tau_{xi} \\ \tau_{yi} \\ \tau_{zi} \end{bmatrix} \tag{7}$$

where C_i is the 1x6 compliance matrix associated with the theoretical load at nominal sensing frame $\{i\}$. The vector C_i can be obtained in a least-squares sense by

$$C_i = \min_{C_i} \sum_{m=1}^{M} (C_i \cdot L_{i,m} - z_{i,m})^2 \tag{8}$$

where M is the number of samples used for calibration, $L_{i,m}$ is the theoretical load vector for sample m and $z_{i,m}$ is the sensor output corresponding to sensor i for sample m, respectively. Each sample is obtained by moving the manipulator to various configurations for a given external load F.

3.2 Calibration of nominal sensing frame

As mentioned in Section 2, crosstalk is included in the sensor output z_i of joint torque sensor i, and is measured at the nominal sensing frame. Such crosstalk can be compensated by estimating the geometric relationship between the actual and the nominal sensing frames. The method for accomplishing this is detailed below.

As discussed in Fig. 1, the measurement in the actual sensing frame does not include any crosstalk. Then, the relationship between the internal force and torque at the actual sensing frame and the sensor output can be written as

$$z_i = \underbrace{[0 \ \ 0 \ \ 0 \ \ 0 \ \ 0 \ \ \gamma_i]}_{\mathbf{L}_{i'}} \cdot \begin{bmatrix} f_{x_{i'}} \\ f_{y_{i'}} \\ f_{z_{i'}} \\ \tau_{x_{i'}} \\ \tau_{y_{i'}} \\ \tau_{z_{i'}} \end{bmatrix} = \gamma_i \tau_{z_{i'}} \tag{9}$$

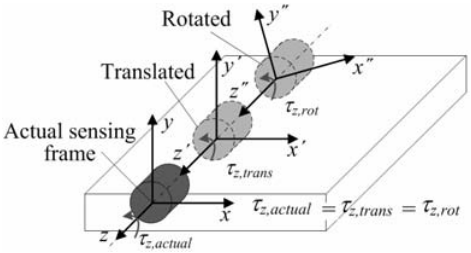

Fig. 3. Sensed torque of actual, translated, and rotated sensing axis.

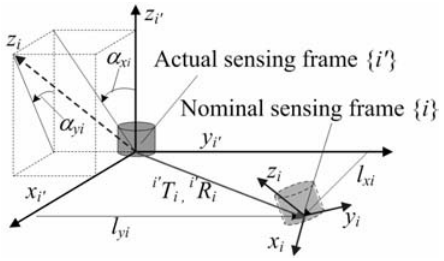

Fig. 4. Geometric relationship between actual and nominal sensing frames.

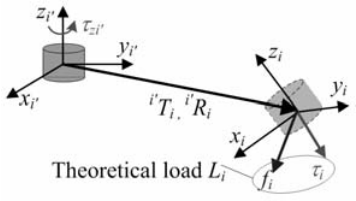

Fig. 5. Sensed torque of actual torque sensor and theoretical load at translated and rotated nominal sensing frame.

where γ_i is the scale factor and $L_{i'}$ is the theoretical load vector written in the actual sensing frame.

Since only z-axis torque is sensed by each torque sensor, the z-axis translation and z-axis rotation of the actual sensing frame relative to the nominal one does not affect the sensor output, as shown in Fig. 3. Therefore, the geometric relationship between the actual and the nominal sensing frames requires description of only 4 parameters representing the translation and rotation about the x-axis and y-axis.

Fig. 4 illustrates the pose (i.e., position and orientation) of nominal sensing frame $\{i\}$ relative to actual sensing frame $\{i'\}$. The four parameters l_{xi}, l_{yi}, α_{xi}, and α_{yi} are used to describe this relationship, as shown in Fig. 4. Therefore, the homogeneous transform matrix ${}^{i'}T_i$ and the rotation matrix ${}^{i'}R_i$ of the nominal sensing frame relative to the actual sensing frame can be obtained by

$${}^{i'}T_i = \mathrm{Trans}(l_{x_i}, l_{y_i}, 0)\,\mathrm{Rot}(y, \alpha_{y_i})\,\mathrm{Rot}(x, \alpha_{x_i}) \tag{10}$$

$$\begin{aligned} {}^{i'}R_i &= \mathrm{Rot}(y, \alpha_{y_i}) \cdot \mathrm{Rot}(x, \alpha_{x_i}) \\ &= \begin{bmatrix} \cos\alpha_{y_i} & \sin\alpha_{x_i}\sin\alpha_{y_i} & \cos\alpha_{x_i}\sin\alpha_{y_i} \\ 0 & \cos\alpha_{x_i} & -\sin\alpha_{x_i} \\ -\sin\alpha_{y_i} & \sin\alpha_{x_i}\cos\alpha_{y_i} & \cos\alpha_{x_i}\cos\alpha_{y_i} \end{bmatrix} \end{aligned} \tag{11}$$

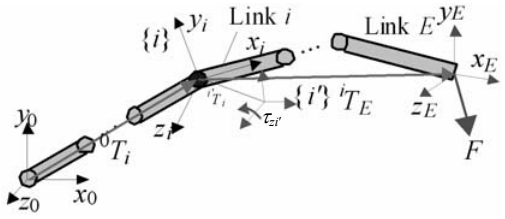

Fig. 6. Joint coordinates of serial manipulator.

The theoretical load $\tau_{zi'}$ in the actual sensing frame and $[f_i\ \tau_i]^T$ in the nominal sensing frame can be described by

$$\tau_{z_{i'}} = [0\ 0\ 1]\,{}^{i'}R_i \begin{bmatrix} \tau_{x_i} \\ \tau_{y_i} \\ \tau_{z_i} \end{bmatrix} + [-l_{y_i}\ l_{x_i}\ 0]\,{}^{i'}R_i \begin{bmatrix} f_{x_i} \\ f_{y_i} \\ f_{z_i} \end{bmatrix} \tag{12}$$

From (7), (9), and (12), the scale factor and four parameters can be expressed in terms of the components of the compliance matrix as follows:

$$\gamma_i = \sqrt{{C_{\tau_{xi}}}^2 + {C_{\tau_{yi}}}^2 + {C_{\tau_{zi}}}^2} \tag{13}$$

$$\alpha_{x_i} = \text{atan2}(C_{\tau_{yi}}, C_{\tau_{zi}}) \tag{14}$$

$$\alpha_{y_i} = \text{atan2}(-C_{\tau_{xi}}, \sqrt{{C_{\tau_{yi}}}^2 + {C_{\tau_{zi}}}^2}) \tag{15}$$

$$l_{x_i} = \frac{1}{\gamma_i}\left(C_{f_{yi}} \cos\alpha_{x_i} - C_{f_{zi}} \sin\alpha_{x_i}\right) \tag{16}$$

$$\begin{aligned} l_{y_i} = -\frac{1}{\gamma_i}(&C_{f_{xi}} \cos\alpha_{y_i} + C_{f_{yi}} \sin\alpha_{x_i} \cos\alpha_{y_i} \\ &+ C_{f_{zi}} \cos\alpha_{x_i} \sin\alpha_{y_i}) \end{aligned} \tag{17}$$

Therefore, the torque without crosstalk in the actual sensing frame can be obtained from (9) and (13). Furthermore, substitution of the four parameters given by (14)-(17) into (10) yields the homogeneous transform matrix between the two frames.

3.3 Calculation of Jacobian matrix

The estimation of the external force applied to the end-effector of a manipulator can be obtained by torque sensing at the actual sensing frame, as shown in Fig. 6.

In general, if each joint torque at the nominal sensing frame is known, the external load of the end-effector can be given by

$$F = \left(JJ^T\right)^{-1} J \cdot \tau \tag{18}$$

where J is the manipulator Jacobian matrix written in the nominal sensing frame. Since the actual sensing frame does not coincide with the nominal sensing frame, the Jacobian matrix written in the actual sensing frame is needed to estimate the external force from the torques measured in the actual sensing frame. By using the homogeneous transform matrix ${}^{i'}T_i$ of the nominal sensing frame relative to the actual sensing frame and the Paul algorithm [14], the Jacobian matrix written in the actual sensing frame can be obtained by

$$\frac{\partial {}^0T_E}{\partial \theta_i} = {}^0T_i\, \Delta_i\, {}^iT_E = \begin{bmatrix} \dfrac{\partial {}^0R_E}{\partial \theta_i} & \dfrac{\partial {}^0r_E}{\partial \theta_i} \\ 0 & 1 \end{bmatrix} \tag{19}$$

where θ_i is the rotation angle of the nominal sensing axis in the direction of the z_i-axis, ${}^0T_i$ is the homogeneous transform of $\{i\}$ relative to $\{0\}$, ${}^iT_E$ is the homogeneous transform of $\{E\}$ relative to $\{i\}$, Δ_i is the differential transformation of the nominal sensing frame $\{i\}$, ${}^0r_E$ is the 3x1 position vector of the end-effector relative to $\{0\}$, and ${}^0R_E$ is the 3x3 rotation matrix of the end-effector relative to $\{0\}$.

Eq. (19) can be expressed with respect to the differential transformation $\Delta_{i'}$ of the actual sensing frame

$$\begin{aligned} \frac{\partial {}^0T_E}{\partial \psi_i} &= {}^0T_{i'}\, \Delta_{i'}\, {}^{i'}T_E = {}^0T_i ({}^{i'}T_i)^{-1} \cdot \Delta_{i'} \cdot {}^{i'}T_i\, {}^iT_E \\ &= \begin{bmatrix} \dfrac{\partial {}^0R_E}{\partial \psi_i} & \dfrac{\partial {}^0r_E}{\partial \psi_i} \\ 0 & 1 \end{bmatrix} \end{aligned} \tag{20}$$

where ψ_i is the rotation angle of the actual sensing axis in the direction of the $z_{i'}$-axis .

Since the differential transformation $\Delta_{i'}$ of the actual sensing frame is relative to the $z_{i'}$-axis, it can be described by

$$\Delta_{i'} = \lim_{\psi_i \to 0} \frac{d\,\text{Rot}(z_{i'}, \psi_i)}{d\psi_i} = \begin{bmatrix} 0 & -1 & 0 & 0 \\ 1 & 0 & 0 & 0 \\ 0 & 0 & 0 & 0 \\ 0 & 0 & 0 & 0 \end{bmatrix} \tag{21}$$

Obtaining all components of the matrix of (20) from (21), the Jacobian matrix written in the actual sensing frame J' is given by

$$J' = \begin{bmatrix} \dfrac{\partial {}^0r_E}{\partial \psi_1} \cdots \dfrac{\partial {}^0r_E}{\partial \psi_E} \end{bmatrix} \tag{22}$$

Finally, the external force applied to the end-effector can be calculated from (9), (18), and (22) as follows:

$$F = \left(J'J'^T\right)^{-1} J' \cdot \tau_{z'} \tag{23}$$

where $\tau_{z'}$ is the torque vector written in the actual sensing frame of each joint.

3.4 Overall calibration process

In this paperr, a novel calibration method is proposed to eliminate the error due to crosstalk. Fig. 7 illustrates the overall procedure of the proposed calibration scheme. The shaded box (measurement process) is the real-time process for sens-

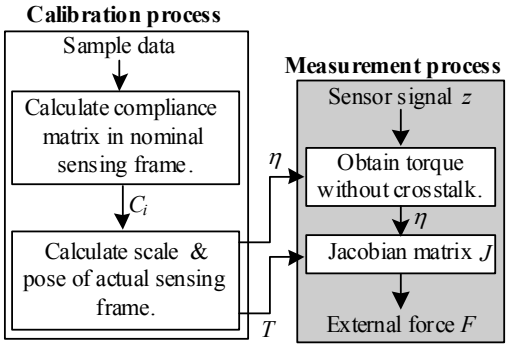

Fig. 7. Sensor calibration method using actual sensing frame.

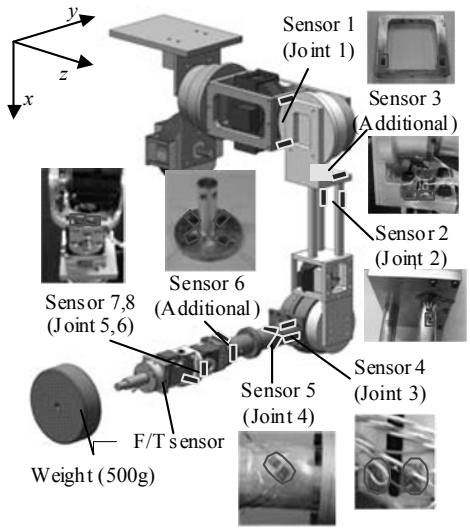

Fig. 8. Bonding positions of strain gauges in 6-DOF manipulator.

ing of the external load, and the transparent box (calibration process) represents the calibration. Both processes were detailed in the previous sections.

4. Experimental verification

To verify the validity of the proposed calibration method, the 6-DOF manipulator shown in Fig. 8 was constructed. This manipulator has a payload of 1kg. The strain gauges were properly bonded to each sensing frame to measure the torques. The bonding positions were carefully determined by FEM analysis. Each joint axis of the manipulator was considered as a nominal sensing axis. Additional two torque sensors were installed for more accurate measurement of the external force.

To obtain sample data for calibration, a 500g weight was attached to the end-effector. The sensor outputs and joint angles for various manipulator configurations were measured. Additionally, to verify the accuracy of the proposed calibration method, the data measured from the commercial 6-axis force/torque sensor (Mini45 model of ATI) installed at the end-effector were compared with those obtained from the proposed calibration method.

In this experiment, 400 dada samples were collected for

Table 1. Compliance matrix of nominal sensing elements.

Sensor	C_{fx}	C_{fy}	C_{fz}	$C_{\tau x}$	$C_{\tau y}$	$C_{\tau z}$	Crosstalk (%)
1	29	-13	0	-50	4	368	14
2	-3	43	-9	780	-112	438	178
3	17	-79	8	39	46	2019	4
4	40	15	-22	177	100	1523	12
5	19	13	2	-104	1	3402	3
6	3	-33	-417	1251	222	-459	273
7	28	876	-45	2640	146	10768	25
8	4	-6	2	-35	12	-537	7

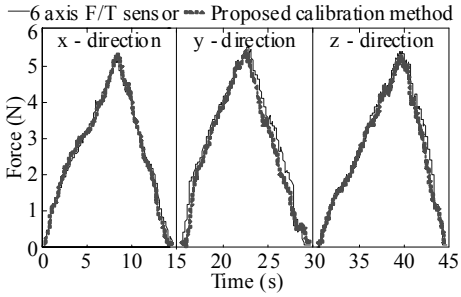

Fig. 9. Force measured by commercial 6-axis F/T and proposed calibration method.

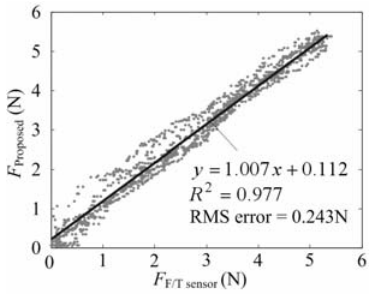

Fig. 10. Least-squares fit of 6-axis F/T sensor vs. calibration method.

various manipulator configurations. Substituting these samples into (8) yielded the compliance matrix shown in Table 1.

The crosstalk error of each sensor can be calculated from these elements of the compliance matrix. Since the z-axis torque of each sensor must be measured, the crosstalk ratio can be defined by the ratio of $C_{\tau z}$ to the other elements (C_{fx}, C_{fy}, C_{fz}, $C_{\tau x}$, and $C_{\tau y}$) of the compliance matrix. In the case of sensor 5, a crosstalk ratio of 3% affects the sensor output. However, the crosstalk ratio of sensor 6 rises to 273%. Using the above compliance matrix of each sensor, the calibration process is conducted.

The scale factor (γ) and the four parameters (i.e., l_x, l_y, α_x, α_y) used to describe the geometrical relationship between the nominal and the actual sensing frames for each sensor can be obtained from (13)-(17). The external load applied to the end-effector can be estimated by substituting these parameters into (23).

To analyze the accuracy of the proposed calibration method,

the external force was applied to the end-effector of the manipulator in the *x*, *y* and *z* directions. In each case, the external force was gradually increased to as high as 5N, after which it was decreased to zero. Fig. 9 shows the comparison of the external forces measured by the proposed calibration method with those measured by the 6-axis F/T sensor. In all directions, the force outputs obtained by the proposed method are in good agreement with those measured by the F/T sensor.

Subsequent experiments were conducted by extending the external force within the range of 0 to 5N in arbitrary directions. Fig. 10 illustrates the 1500 sensor output data obtained by the proposed method and the F/T sensor. The RMS of the sensing error of the proposed calibration method, computed over the entire sensing range, is 0.243N. Since the RMS of the error is below 5% of the full sensing range, the performance of the proposed calibration method could be verified as similar to that of the 6-axis commercial F/T sensor.

5. Conclusion

In this paper, a novel calibration method for coping with torque sensor crosstalk was proposed. When this method is applied to a sensor for which there is considerable crosstalk, reliable measurement can be achieved. Since the location of the actual sensing frame can be computed by the proposed calibration scheme, rather inaccurate installation of the torque sensor at the manipulator is tolerable. The proposed calibration scheme can be utilized by means of a known weight without any additional device.

Currently, a gravity compensation algorithm to be integrated with the proposed calibration method is under development.

Acknowledgements

This work was supported by the Center for Autonomous Intelligent Manipulator under Human Resources Development Program for Robot Specialists and by Basic Science Research Program through the National Research Foundation of Korea (No. 2010-0001647).

References

[1] M. Salehi, and G. Vossoughi, Impedance Control of Flexible Base Mobile Manipulator Using Singular Perturbation Method and Sliding Mode Control Law, *Int. Journal of Control, Automation, and Systems*, 6 (5) (2008) 677-688.

[2] A. Pervez, and J. Ryu, Safe Physical Human Robot Interaction-Past, Present and Future, *Journal of Mechanical Science and Technology*, 22 (3) (2008) 469-483.

[3] T. C. Phung, S. H. Ha, Y. S. Ihn, B. J. Choi, S. M. Lee, J. C. Koo, and H. R. Choi, An Enhanced Force and Contact Position Sensor for Micro-Manipulators, *Int. Journal of Control, Automation, and Systems*, 7 (3) (2009) 459-467.

[4] G. S. Kim, The design of a six-component force/moment sensor and evaluation of its uncertainty, *Measurement Science and Technology*, 12 (2001) 1445-1455.

[5] B. E. Shimano, *The Kinematic design and force control of computer controlled manipulators*, Artificial Intelligence Lab., Stanford Univ., AI Memo, 313 (1978).

[6] A. Bicchi, A Criterion for Optimal Design of Multi-axis Force Sensors, *Journal of Robotics and Autonomous Systems*, 10 (4) (1992) 269-286.

[7] M. Richard, J. Voyles, and D. Morrow, Shape from motion approach to rapid and precise force/torque sensor calibration, *Proc. of Int. Mechanical Engineering Congress and Exposition*, 119 (2) (1997) 229-235.

[8] M. Donghai, and M. John, Gravity-based Autonomous Calibration for Robot Manipulators, *Proc. of Int. Conf. on Robotics and Automation*, San Diego, CA, USA (1994) 2763-2768.

[9] B. Kim, and S. Yun, Development of a Joint Torque Sensor Fully Integrated with an Actuator, *Proc. of Int. Conf. on Control, Automation and Systems*, (2005) 1679-1683.

[10] H. D. Taghirad, A. Helmy and P. R. Belanger, Intelligent Built-in Torque Sensor for Harmonic Drive Systems, *Proc. of IEEE Instrumentation and Measurement,* 48 (6) (1999) 969-974.

[11] J. Y. Kim and I. W. Park, System Design and Dynamic Walking of Humanoid Robot KHR-2, *Proc. of IEEE Int. Conf. on Robotics and Automation*, Barcelona, Spain (2005) 1443-1448.

[12] D. Vischer and O. Khtib, Design and Development of High-Performance Torque-Controlled Joints, *IEEE Transactions on Robotics and Automation*, 11 (4) (1995) 537-544.

[13] S. H. Lee, Y. L. Kim and J. B. Song, Torque Sensor Calibration Using Virtual Load for a Manipulator, Int. Journal of Precision Engineering and Manufacturing, 11 (2) (2010) 219-225.

[14] R. P. Paul, Robot Manipulators: Mathematics, Programming, and Control, Cambridge, MA: MIT Press, (1981) 85-108.

Young-Loul Kim received his B.S. degree in Mechanical Engineering from Korea University, in 2007. He is now enrolled in the Integrated Master's & Doctoral course in Mechanical Engineering at Korea University. His research interests include force sensors and motion control.

Jung-Jun Park received his M.S. and Ph.D. degree in Mechanical Engineering from Korea University, in 2005 and 2010, respectively. Dr. Park is currently engaged in postdoctoral work in the School of Mechanical Engineering at Korea University. His research interests include robotic manipulation and safe robot arms.

Jae-Bok Song received his B.S. and M.S. degree in Mechanical Engineering from Seoul National University in 1983 and 1985, respectively. He was awarded his Ph.D. degree from M.I.T. in 1992. Dr. Song is currently a Professor at the School of Mechanical Engineering at Korea University. He has served as a director of Intelligent Robotics Laboratory from 1993. Dr. Song's research interests include safe manipulators, design and control of robotic systems, and indoor/outdoor navigation.